cm^{-1}, $^3A_{2g}(^3G)$ expected at approximately 18 000 cm^{-1}, $^3A_{1g}(^3H)$ expected at approximately 18 500 cm^{-1}, $^3B_{1g}(^3F)$ expected at approximately 20 500 cm^{-1}, and $^3B_{2g}(^3D)$ expected above 22 000 cm^{-1}. Besides the two $^3B_{1g}$ excitations dominating the A_2CrX_4 spectrum, there are two additional transitions in the 16 000–20 000-cm^{-1} energy range that are expected to gain intensity by the Tanabe mechanism. This is in very nice agreement with the observed richness of the absorption spectrum in this spectral range. The sharpness of the absorption bands clearly identifies them as intraconfigurational transitions. The band system just above 16 000 cm^{-1} in the spectrum of $CrCl_2$ has the wrong polarization to be assigned to $^3B_{1g}$. The band near 17 000 cm^{-1}, with predominant polarization parallel to the chain axis, is a much more likely candidate for the $^3B_{1g}(^3H)$ excitation. We attribute this shift of the $^3B_{1g}(^3H)$ energy to the larger tetragonal crystal field and slightly larger electron repulsion parameters in $CrCl_2$. This is also reflected in the significantly higher energy of the $^5A_{1g}(E_g)$ transition compared to that of TMCC and $(C_2H_5NH_3)_2CrCl_4$ (section 3).

The visible spectra of TMCC and $CsCrCl_3$ are similar in appearance to that of $CrCl_2$. A detailed analysis in terms of intensity-gaining orbital mechanisms is complicated by the crystal structure. It is evident, from Figure 5, however, that overlap and thus electron-transfer pathways do exist between neighboring Cr^{2+} ions in the chains. The situation is therefore comparable to that for $CrCl_2$, and the exchange mechanism provides intensity for several transitions in the 16 000–22 000-cm^{-1} range. The polarizations of the bands centered near 16 000 and 19 000 cm^{-1} are compatible with $^3B_{1g}$ excitations, and by analogy with the A_2CrCl_4 spectra we assign them accordingly. The 19 000-cm^{-1} band is possibly a superposition of $^3B_{1g}(^3F)$ and $^3A_{1g}(^3H)$. It therefore appears that the two $^3B_{1g}$ transitions have very similar energies in TMCC and $(C_2H_5NH_3)_2CrCl_4$. This is in good agreement with our conclusion from the $^5A_{1g}(E_g)$ band that the tetragonal crystal field and the electron repulsion parameters are very similar in these compounds. In all our compounds the actual point symmetry at the Cr^{2+} sites is lower than D_{4h}. This, together with spin–orbit coupling, leads to additional splittings and thus increases the number of observed transitions. A fit of calculated crystal field energies to the experimental band positions is not meaningful. The observed strong polarization of some of the bands in the $ACrX_3$ and $CrCl_2$ spectra restricts the possible excited states, but we feel that assignments of all the individual bands would be hazardous.

The striking observation, however, that the $ACrX_3$ and $CrCl_2$ spectra are much richer than the A_2CrX_4 spectra in the range 16 000–22 000 cm^{-1} can now be understood. It is due to the lack of overlap between magnetic orbitals on neighboring Cr^{2+} ions in A_2CrX_4, as discussed above. In $ACrX_3$ and $CrCl_2$, on the other hand, the relative dispositions of magnetic orbitals on neighboring Cr^{2+} ions is more favorable for overlap. This is a direct result of the crystal structures, the bridging geometry between nearest neighbors, in particular. These pathways lead to antiferromagnetic kinetic exchange on the one hand and to exchange-induced intensity for spin-forbidden excitations on the other. Spin flips in the relevant orbitals lead to several excited states that are spectroscopically accessible. It is thus clear that the ferromagnetism and the small number of spin-forbidden bands in the compounds A_2CrX_4 have a common origin: lack of overlap between singly occupied orbitals on neighboring Cr^{2+} ions.

Acknowledgment. We thank S. Patrizio for technical assistance. This work was financially supported by the Consiglio Nazionale delle Ricerche and the Swiss National Science Foundation.

Registry No. $(CH_3)_4NCrBr_3$, 29794-92-1; $(CH_3)_4NCrCl_3$, 29794-88-5; $CsCrCl_3$, 13820-84-3; $CrCl_2$, 10049-05-5; $(C_2H_5NH_3)_2CrCl_4$, 62212-04-8; $(C_2H_5NH_3)_2CrBr_4$, 63949-50-8.

Contribution from the Department of Chemistry, North Carolina State University, Raleigh, North Carolina 27695-8204

Spectroelectrochemical Properties of Ruthenium(II) Tris Chelate Complexes of 2,2′-Bipyrimidine and 2,2′-Bipyrazine

C. D. Tait, R. J. Donohoe,† M. K. DeArmond, and D. W. Wertz*

Received February 18, 1987

The electronic absorption and resonance Raman (RR) spectra of the reduction products of $[Ru(bpm)_3]^{2-n}$ and mixed-ligand complexes $[Ru(bpz)_x(bpy)_{3-x}]^{2-n}$ ($x = 1-3$, $n = 0-3$) are discussed, as well as the low-temperature electron spin resonance (ESR) spectrum of $[Ru(bpz)_3]^0$ (bpm = 2,2′-bipyrimidine, bpz = 2,2′-bipyrazine, and bpy = 2,2′-bipyridine). The ultraviolet (UV) absorption and RR spectra for the reduction products of the tris(bipyrimidine) complex are analogous to those of the tris(bipyridine) complex and argue strongly for a localized redox orbital description. While the ESR and near-IR (near-infrared) absorption spectra also argue for localized redox orbitals in the bpz complexes, the simple $(bpz)_{3-n}/(bpz^-)_n$ $\pi \rightarrow \pi^*$ chromophoric behavior typical in the UV absorption spectrum is not observed. Furthermore, there is a gradual shifting of the RR peaks as electrons are added, with no distinct vibrational pattern from reduced and unreduced bipyrazine ligands for the one- and two-electron-reduction products as seen in the complexes of $[Ru(bpy)_3]^{2-n}$ and $[Ru(bpm)_3]^{2-n}$.

Introduction

The recognition of redox orbital localization within a single ligand in d^6 metal tris(diimines)[1-3] has prompted investigation into the mechanism behind the molecular symmetry lowering. One method of such an investigation involves varying the ligands around the metal center, and to that end some or all of the archetypical bipyridine (bpy) ligands in $Ru(bpy)_3^{2+}$ have been replaced with bipyrimidine (bpm) and bipyrazine (bpz) ligands. As is evident from the molecular structures for these ligands shown in Figure 1, this is equivalent to replacing with nitrogens the C–H moieties meta to the coordinating nitrogens for bipyrimidine and para to the coordinating nitrogens for bipyrazine. Because nitrogen is more electronegative than the carbon it replaces, the π orbitals would be expected to be lower in energy for the hetero ligands than for bpy, which could result in greater mixing of the lower energy redox orbitals with the metal orbitals through π backbonding. While the cyclic voltammetric data reported for the bpz complex[4-7] and the bpm complex[7-9] do indeed indicate the redox

†Present address: Department of Chemistry, Carnegie-Mellon University, Pittsburgh, PA 15213.

(1) Vlcek, A. A. *Coord. Chem. Rev.* **1982**, *43*, 39.
(2) DeArmond, M. K.; Hanck, K. W.; Wertz, D. W. *Coord. Chem. Rev.* **1985**, *64*, 65.
(3) Braterman, P. S.; Heath, G. A.; Yellowlees, L. J. *J. Chem. Soc., Dalton Trans.* **1985**, 1081.
(4) Crutchley, R. J.; Lever, A. B. P. *Inorg. Chem.* **1982**, *21*, 2276.
(5) Gonzales-Velasco, J.; Rubinstein, I.; Crutchley, R. J.; Lever, A. B. P.; Bard, A. J. *Inorg. Chem.* **1983**, *22*, 822.

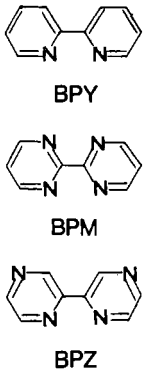

Figure 1. Molecular structures of the ligands used in this study: bpy = 2,2′-bipyridine, bpm = 2,2′-bipyrimidine, bpz = 2,2′-bipyrazine.

orbitals are lower in energy than those of the bipyridine complex, the lower basicity, especially of bpz, has been shown to result in weaker metal–ligand bonding and to negate the tendency toward increased π back-bonding for the unreduced complexes.[4] In addition, the replacement of a peripheral hydrogen by a lone pair of electrons might be expected to change the solvation properties of the complex, where solvation has been implicated in the localization mechanism.[10-12]

The exposed sp^2 lone pair on the nitrogens of bpm can also be used to coordinate a second ruthenium metal–ligand center,[7,13-18] while those of the bpz ligand can form multiple-metal complexes.[19] With two metal centers present, the new system is more favorably disposed toward the transference of electrons in multiples of two (one from each metal center) sought for the use of metal diimine systems in the photoreduction of water.[20] An investigation of the properties of the monomer subunits, then, serves as a preliminary step in the investigation of these bimetallic systems as well as an investigation of the redox localization mechanism.

Experimental Section

The bpy and bpm ligands were purchased from Aldrich and Alfa, respectively, while the bpz ligand was prepared by published procedures,[4,21] as were the tris complexes $[Ru(bpm)_3][PF_6]_2$ and $[Ru(bpz)_3][PF_6]_2$.[4,14] The mixed bpy–bpz ruthenium complexes were synthesized by first making the dichloride bis(diimine) complex, purifying the intermediate, and then adding the third ligand as described elsewhere.[22] The ligands were repeatedly recrystallized from toluene, while the complexes were purified on a Sephadex LH-20 column in acetone and recrystallized from acetone–diethyl ether. The identity of the complexes was checked by comparing the cyclic voltammograms (CV) and absorption spectra with those in the literature,[4,7,14] and the purity was verified by an emission spectrum independent of excitation wavelength.

The purifications of the supporting electrolyte tetrabutylammonium hexafluorophosphate (TBAH) and solvents (dimethylformamide (DMF) and dimethyl sulfoxide (Me_2SO)) were performed as reported elsewhere.[6] Electrochemical and spectroscopic methods have also been described previously.[23-26] Sample integrity was monitored throughout the measurements by rechecking the CV against that obtained for the starting material. Because of photodecomposition at room temperature,[27,28] the RR (resonance Raman) spectra of unreduced $Ru(bpm)_3^{2+}$ and $Ru(bpz)_3^{2+}$ were also taken at 77 K to ensure that the RR spectra obtained were indeed from the stated complexes. All RR peaks are reported against the 865-cm^{-1} DMF solvent peak or the 955-cm^{-1} Me_2SO solvent peak, as measured against the 865-cm^{-1} DMF peak in a mixed-solvent test for self-consistency. The monochromator slits were set for 5-cm^{-1} resolution, and the frequencies were measured with an uncertainty of ± 2 cm^{-1} for strong, well-resolved peaks. The ESR measurements were carried out on the reduced complex in sealed quartz capillary tubes in an IBM ER200 series spectrometer equipped with an Air Products low-temperature controller and cryotip.

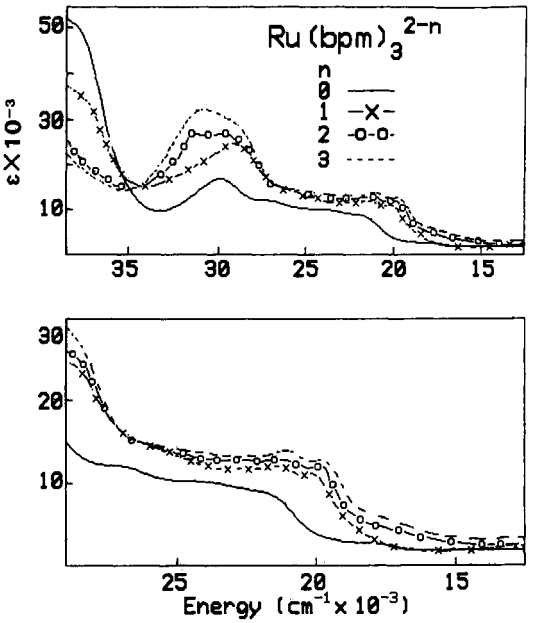

Figure 2. Electronic absorption spectrum of $[Ru(bpm)_3]^{2-n}$ in DMF, where n is the number of electrochemically added electrons. The lower spectrum expands the congested visible region.

Results and Discussion

I. Absorption Spectra. A. $[Ru(bpm)_3]^{2-n}$ (n = 0–3). From the UV–vis absorption spectrum for the unreduced complex shown in Figure 2, the strong absorption at high energies associated with a ligand-based $\pi \rightarrow \pi^*$ transition[7] does not reach its peak before the UV cutoff of the solvent (DMF) is reached. As electrons are added, this absorption decreases in intensity, but not with the constant loss expected for the presence of three separate chromophores characteristic of species with localized redox orbitals. However, only the low-energy part of the absorption is observed, and other absorptions at slightly higher energy than the $\pi \rightarrow \pi^*$ bands may be red-shifting as electrons are added, eventually appearing within the spectral range as an absorption tail. Such red-shifting of bands as electrons are added frequently occurs and is not unexpected. While the $\pi \rightarrow \pi^*$ absorption is decreasing in intensity, a new absorption at $\sim$32 000 cm^{-1} appears and is assigned, by analogy to the redox absorption behavior of $[Ru(bpy)_3]^{2-n}$,[29] to a reduced ligand-based bpm^- absorption. Its relatively constant increase in intensity with each added electron is

(6) Ohsawa, Y.; Hanck, K. W.; DeArmond, M. K. *J. Electroanal. Chem. Interfacial Electrochem.* **1984**, *175*, 229.
(7) Rillema, D. P.; Allen, G.; Meyer, T. J.; Conrad, D. *Inorg. Chem.* **1983**, *22*, 1617.
(8) Watanabe, J.; Saji, T.; Aoyagui, S. *Bull. Chem. Soc. Jpn.* **1982**, *55*, 327.
(9) Kawanishi, Y.; Kitamura, N.; Kim, Y.; Tazuke, S. *Sci. Pap. Inst. Phys. Chem. Res. (Jpn.)* **1984**, *78*(4), 212.
(10) Yersin, H.; Gallhuber, E. *J. Am. Chem. Soc.* **1984**, *106*, 6582.
(11) Ferguson, J.; Krausz, E. *Chem. Phys. Lett.* **1986**, *127*, 551.
(12) Kitamura, N.; Kim, H.-B.; Kawanishi, Y.; Obata, R.; Tazuke, S. *J. Phys. Chem.* **1986**, *90*, 1488.
(13) Lin, C.-T.; Bottcher, W.; Chou, M.; Creutz, C.; Sutin, N. *J. Am. Chem. Soc.* **1976**, *98*, 6536.
(14) Hunziker, M.; Ludi, A. *J. Am. Chem. Soc.* **1977**, *99*, 7370.
(15) Dose, E. V.; Wilson, L. J. *Inorg. Chem.* **1978**, *17*, 2660.
(16) Ruminski, R. R.; Petersen, J. D. *Inorg. Chem.* **1982**, *21*, 3706.
(17) Rillema, D. P.; Mack, K. B. *Inorg. Chem.* **1982**, *21*, 3849.
(18) Goldsby, K. A.; Meyer, T. J. *Inorg. Chem.* **1984**, *23*, 3002.
(19) Toma, H. E.; Lever, A. B. P. *Inorg. Chem.* **1986**, *25*, 176.
(20) McLendon, G. In *Energy Resources through Photochemistry and Catalysis*; Gratzel, M., Ed.; Academic: New York, 1983.
(21) Currently available commercially from Aldrich.
(22) Tait, C. D.; Vess, T. M.; DeArmond, M. K.; Hanck, K. W.; Wertz, D. W. *J. Chem. Soc., Dalton Trans.*, in press.
(23) Morris, D. E.; Hanck, K. W.; DeArmond, M. K. *J. Electroanal. Chem. Interfacial Electrochem.* **1983**, *149*, 115.
(24) Morris, D. E.; Hanck, K. W.; DeArmond, M. K. *J. Am. Chem. Soc.* **1983**, *105*, 3032.
(25) Angel, S. M.; DeArmond, M. K.; Donohoe, R. J.; Hanck, K. W.; Wertz, D. W. *J. Am. Chem. Soc.* **1984**, *106*, 3688.
(26) Angel, S. M.; DeArmond, M. K.; Donohoe, R. J.; Wertz, D. W. *J. Phys. Chem.* **1985**, *89*, 282.
(27) Allen, G. H.; White, R. P.; Rillema, D. P.; Meyer, T. J. *J. Am. Chem. Soc.* **1984**, *106*, 2613.
(28) Kalyanasundaram, K. *J. Phys. Chem.* **1986**, *90*, 2285.
(29) Heath, G. A.; Yellowlees, L. J.; Braterman, P. S. *J. Chem. Soc., Chem. Commun.* **1981**, 287.

Table I. UV Absorption Peaks, in $cm^{-1} \times 10^3$, and Extinction Coefficients (in Parentheses) in M^{-1} cm^{-1}, for the series $[Ru(bpz)_x(bpy)_{3-x}]^{2-n}$ in DMF[a]

	$x = 0$	$x = 1$	$x = 2$	$x = 3$	chromophore
$n = 0$	35.3 (60000)	35.0 (62000)	35.0 (sh)		bpy
		32.4 (sh)	33.4 (55000)	34.2 (6200)	bpz
$n = 1$	35.1 (44000)	34.2 (60000)	34.5 (48000)		bpy
			33.0 (sh)	32.7 (46000)	bpz
	29.4 (15000)				bpy^-
		27.0 (sh)	27.0 (sh)	27.0 (sh)	bpz^-
$n = 2$	33.9 (34000)	33.9 (49000)	34.0 (45000)		bpy
				30.1 (40000)	bpz
			29.9 (30000)		*b*
	29.2 (23000)	29.4 (29000)			bpy^-
			26.8 (20000)	28.0 (sh)	bpz^-
$n = 3$	30.5 (37000)	29.9 (49000)			bpy^-
				30.1 (41000)	*b*
				26.0 (sh)	bpz^-

[a] x is the number of bipyrazine ligands, and n is the number of electrons added. [b] See text.

characteristic of separate ligand chromophore behavior and hence would argue for a localized description of the redox orbital.

For the unreduced complex, the visible region of the spectrum contains two metal-to-ligand charge-transfer (MLCT) transitions into the two lowest ligand-based π^* levels.[7,9,14] As the redox electrons are added to the π^* system of the ligands, the lowest energy MLCT decreases in intensity and, by analogy to other tris(diimine) d^6 metal complexes,[26,29,30-33] red-shifts; meanwhile, reduced ligand-based $\pi^* \rightarrow \pi^*$ transitions gain intensity. After three electrons have been added, thereby resulting in each low-lying π^* orbital being occupied, the lowest MLCT is gone, and the visible spectrum is due solely to the reduced ligand-based transitions. While the UV spectrum suggests that the redox orbitals are best described as localized, the congestion in the visible region does not yield direct evidence for this conclusion; however, it is this spectral region that is probed in the resonance Raman experiments discussed below.

B. $[Ru(bpz)(bpy)_2]^{2-n}$ and $[Ru(bpz)_2(bpy)]^{2-n}$ ($n = 0$–3). The UV region of the spectrum for the mixed-ligand bpz–bpy ruthenium complexes is dominated by the $\pi \rightarrow \pi^*$ absorption of bpy at $\sim 35 \times 10^3$ cm^{-1} and that of bpz at $\sim 33 \times 10^3$ cm^{-1} (Table I). Despite the spectral overlap of these bands, the assignments of these peaks are consistent, in terms of both peak position and intensity trends, with those expected from a weighted sum of the UV peaks of $Ru(bpy)_3^2$ and $Ru(bpz)_3^2$, thereby indicating separate bpy and bpz π systems. The 33×10^3 cm^{-1} absorption is reduced in intensity before the one at 35×10^3 cm^{-1} upon addition of electron(s), consistent with cyclic voltammetric results[7] which predict that the lowest redox orbital is localized in the bpz ligand(s). Upon reduction of the last bpz ligand, the 33×10^{-3} cm^{-1} peak is gone and addition of the next redox electron decreases the intensity of the $(34–35) \times 10^3$ cm^{-1} bpy $\pi \rightarrow \pi^*$ absorption until it is also absent in the triply reduced species. Furthermore, absorptions associated with the reduced ligands generally exhibit monotonic intensity increases: the small absorption at $\sim 27 \times 10^3$ cm^{-1} from bpz^- is apparent after the first electron has been added, while the relatively strong absorption at 29×10^3 cm^{-1} from bpy^-[29] increases as the final electron is added. However, a different peak at 29.9×10^3 cm^{-1} appears for $[Ru(bpz)_2(bpy)]^0$ and will be discussed in the next section.

The two peaks in the visible spectrum of the unreduced complexes have been attributed to MLCT bands, one into bpz (22000 cm^{-1}) and the other into bpy (24000 cm^{-1}).[7] Upon reduction, the MLCT into bpz is replaced by a bpz^--based $\pi^* \rightarrow \pi^*$ visible absorption. Further reduction eliminates the MLCT in bpy while adding bpy^--based adsorption to the visible region (also see resonance Raman section).

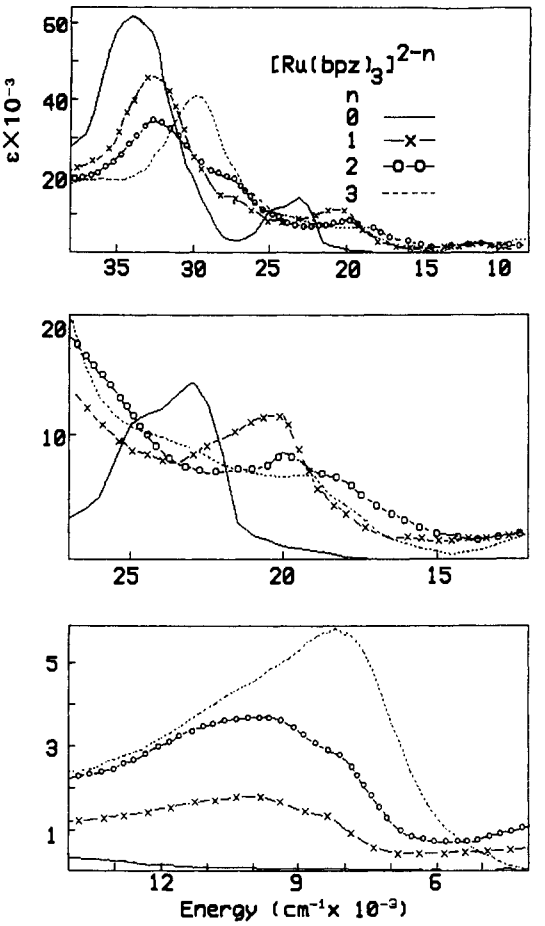

Figure 3. Electronic absorption spectrum of $[Ru(bpz)_3]^{2-n}$ in DMF, where n is the number of electrochemically added electrons. The visible and near-infrared regions are expanded in the lower plots.

C. $[Ru(bpz)_3]^{2-n}$. The spectral behavior for the $n = 1$ and $n = 2$ cases of $[Ru(bpz)_3]^{2-n}$ (Table I and Figure 3) is quite similar to that for the well-described $[Ru(bpy)_3]^{2-n}$ series.[29] The $\pi \rightarrow \pi^*$ band (34200 cm^{-1} for $n = 0$) decreases in intensity as bpz π^* orbitals are filled, the remaining absorption is slightly red-shifted from a Coulombic destabilization of the π electrons, and the weak UV absorption associated with the reduced bpz^- chromophores appears at ~ 27000 cm^{-1}. However, a distinct break in the UV pattern occurs for the third reduction product, where a peak at 30100 cm^{-1} appears that is similar to, but stronger than, the one noted in $[Ru(bpz)_2(bpy)]^0$ ($n = 2$), where the final bpz ligand is also reduced. Its intensity is inconsistent with assigning it to

(30) Elliott, C. M.; Hershenhart, E. J. *J. Am. Chem. Soc.* **1982**, *104*, 7519.
(31) Donohoe, R. J.; Tait, C. D.; DeArmond, M. K.; Wertz, D. W. *Spectrochim. Acta, Part A* **1986**, *42A*, 233.
(32) Donohoe, R. J.; Tait, C. D.; DeArmond, M. K.; Wertz, D. W. *J. Phys. Chem.* **1986**, *90*, 3923.
(33) Donohoe, R. J.; Tait, C. D.; DeArmond, M. K.; Wertz, D. W. *J. Phys. Chem.* **1986**, *90*, 3927.

the same transition previously associated with the bpz^- absorption, and the persistence of the bpz^- absorption shoulder at 27×10^3 cm^{-1} also argues against its being due to the addition of a similar, third reduced chromophore.

The visible portion of the spectrum is dominated by the metal-to-ligand charge-transfer (MLCT) band in the $n = 0$ and $n = 1$ species.[4,7,34] As electrons are added, this band diminishes in intensity and shifts to lower energy (due to a Coulombic destabilization of the occupied d orbitals) to be replaced by $\pi^* \rightarrow \pi^*$ transitions for the highly reduced species.

Because of the anomalous behavior in the absorption spectra of $[Ru(bpz)_3]^{2-n}$, the near-infrared (near-IR) absorption region was examined in more detail. A weak absorption ($\epsilon < 1000$ M^{-1} cm^{-1}) for the singly and doubly reduced species extends to energies lower than 4000 cm^{-1}, below which solvent overtones precluded continuance of the spectrum. This low-energy absorption is absent in the spectra of the unreduced and reduced free ligand, as well as the unreduced and triply reduced ruthenium complex. By analogy to other complexes,[22,35,36] this lower energy absorption may be associated with an intervalence charge-transfer (IVCT) band. Such an absorption would only occur in type II species of the Robin–Day classification of mixed-valence compounds[37-39] and would imply that an electron is optically excited from a reduced ligand to an unreduced ligand on the same complex. For a weakly coupled system, this optical energy should be 4 times higher than the barrier to the corresponding thermal electron transfer. Recently, an activation energy of ~ 720 cm^{-1} for thermal electron hopping has been determined by a temperature-dependent line-broadening ESR study of $[Ru(bpz)_3]^{1+}$,[40] predicting an IVCT centered at ~ 3000 cm^{-1} and possibly corresponding to the weak near-IR absorption seen here. The existence of an IVCT, then, would imply both reduced and unreduced ligands on the same complex and hence a localized redox orbital description for the reduction products $n = 1$ and $n = 2$, as suggested in the ESR experiment.[40] However, the optical evidence is not compelling since the absorption, besides being the weakest in the spectral range studied, does not reach a peak, leaving its position and width undetermined: its absence in the triply reduced complex may be a consequence of peak shifting and/or line narrowing in a delocalized orbital description.

II. Resonance Raman (RR) Spectra. Resonance Raman spectroscopy of reduced diimine d^6 metal complexes has been used previously to characterize the nature of the redox orbital.[25] In the localized limit for the $n = 1$ and $n = 2$ reduction products, the spectrum of the unreduced ligand, a fully reduced ligand, or a composite of the two will be observed depending on whether Raman excitation is into the MLCT, $\pi^* \rightarrow \pi^*$, or a region of overlap. In the delocalized limit, the spectrum of only one type of vibrational unit will be observed: one with vibrational frequencies between those observed in the unreduced and fully reduced limits since the redox electrons will be shared equally by the equivalent ligands. The relative intensities of the peaks, however, might be expected to change, since enhancement, initially from the MLCT absorption band, will be exclusively from the $\pi^* \rightarrow \pi^*$ transition in the three-electron reduction and some mixture of the two for the intermediate cases.

A. $[Ru(bpm)_3]^{2-n}$ ($n = 0$–4). The resonance Raman spectra between 850 and 1650 cm^{-1} for the reduction products of the tris(bipyrimidine) complex are shown in Figure 4, with the $n = 0$ and $n = 3$ spectra showing the vibrational spectra of an unreduced and fully reduced bpm ligand, respectively. The Raman

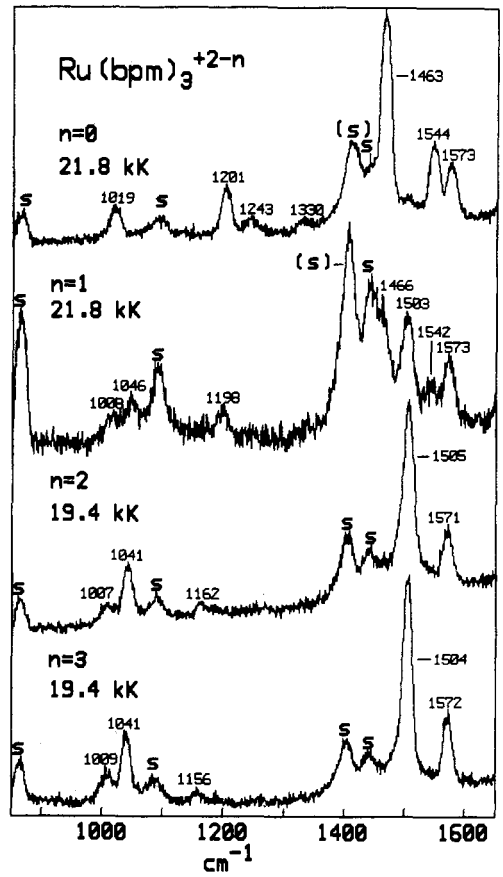

Figure 4. Resonance Raman spectra for the reduction products of $[Ru(bpm)_3]^{2-n}$ in DMF. The excitation energy is noted just above each spectrum (1 kK = 1000 cm^{-1}; S = solvent peak).

spectrum of the first reduction product with excitation at 21.8 $\times 10^3$ cm^{-1} clearly shows a superposition of peaks associated with bpm (e.g. 1466, 1542, and 1198 cm^{-1}) and bpm^- (e.g. 1046 and 1503 cm^{-1}), requiring the simultaneous existence of both bpm and bpm^- within the same complex and hence requiring a localized redox orbital description since in the delocalized case, three equivalent $bpm^{1/3-}$ would exist. Scattering of lower frequency laser excitation (19.4×10^3 cm^{-1}) for both the first and second reduction products yields spectra similar to the one shown for the $n = 2$ case in Figure 5 and reveals peak identical, within experimental error, with those associated with fully reduced ligands. Therefore, fully reduced ligands exist in the one- and two-electron-reduction products, consistent with a localized redox orbital description, and the absorption in the lower energy region of the visible spectrum can be assigned as a $\pi^* \rightarrow \pi^*$ bpm^--based absorption. The resonance Raman spectrum for the four-electron-reduction product also gave a vibrational spectrum associated with the presence of the bpm^- ligand, implying that this fourth electron is not shared between the ligands but is also localized on only one of the ligands. The resonance Raman spectra for the redox series of $[Ru(bpm)_3]^{2-n}$, then, gives compelling evidence for the localization of added electron density into single ligands through the first four added electrons. That the redox orbitals are localized is consistent with a previous finding that the optical orbital (i.e. final ligand orbital in the MLCT) for the bpm compound is also localized.[41]

B. $[Ru(bpz)(bpy)_2]^{2-n}$ ($n = 0$–3). The previous assignment for the two absorption bands in the visible spectrum for the unreduced ($n = 0$) complex as two MLCT[7] bands was verified from the RR results. Excitation into the one at lower energy (20.5×10^3 cm^{-1}) produced a vibrational spectrum similar to the one found for the $(bpz)_3$ complex (see ref 42 and Figure 6) and hence agreed with

(34) Venturi, M.; Mulazzani, Q. G.; Ciano, M.; Hoffman, M. Z. *Inorg. Chem.* **1986**, *25*, 4493.
(35) Tait, C. D.; MacQueen, D. B.; Donohoe, R. J.; DeArmond, M. K.; Hanck, K. W.; Wertz, D. W. *J. Phys. Chem.* **1986**, *90*, 1766.
(36) Heath, G. A.; Yellowlees, L. J.; Braterman, P. S. *Chem. Phys. Lett.* **1982**, *92*, 646.
(37) Robin, M. B.; Day, P. *Adv. Inorg. Chem. Radiochem.* **1967**, *10*, 247.
(38) Piepho, S. B.; Krausz, E. R.; Schatz, P. N. *J. Am. Chem. Soc.* **1978**, *100*, 2996.
(39) Launay, J. P.; Babonneau, F. *Chem. Phys.* **1982**, *67*, 295.
(40) Gex, J.-N.; DeArmond, M. K.; Hanck, K. W. *J. Phys. Chem.* **1987**, *91*, 251.
(41) Akasheh, T. S.; Beaumont, P. C.; Parsons, B. J.; Phillips, G. O. *J. Phys. Chem.* **1986**, *90*, 5651.

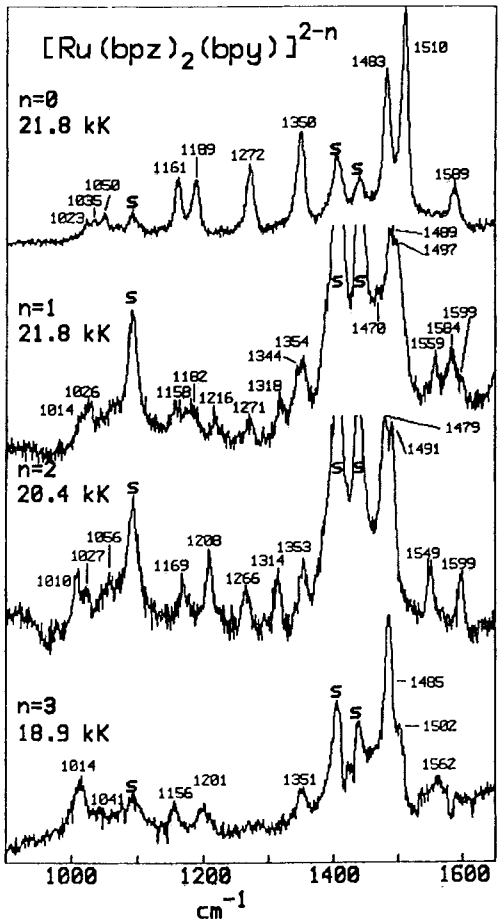

Figure 5. Resonance Raman spectra for the reduction products of the mixed-ligand $[Ru(bpz)_2(bpy)]^{2-n}$ in DMF (1 kK = 1000 cm^{-1}; S = solvent peak).

the metal-to-bpz assignment of this absorption. Furthermore, by excitation at higher energy (21.8×10^3 cm^{-1}) the vibrational spectrum of bpy, as shown by the presence of peaks at 1601, 1555, and 1319 cm^{-1}, began to be superimposed onto the bpz spectrum, consistent with some enhancement from the higher energy absorption tail associated with a metal-to-bpy charge transfer. After the addition of one electron, the 21.8×10^3 cm^{-1} excitation gave a relatively strong bpy vibrational spectrum, indicating a red shift in the metal-to-bpy charge-transfer band. Scattering from 20.1 $\times 10^3$ cm^{-1} laser irradiation still gave evidence of bpy but also produced a strong peak at 1211 cm^{-1} associated with bpz^- (see below), consistent with initial reduction of the bpz ligand. Raman spectra of the two-electron product yielded evidence for bpy, bpy^- (1507 and 1353 cm^{-1}), and bpz^-, with the bpz^- vibrations receiving more enhancement at lower excitation energies (e.g. 18.9×10^3 cm^{-1}). The presence of bpy^- vibrations is direct verification of the previous interpretation[7] of the second wave of the cyclic voltammogram as being due to bipyridine reduction rather than spin pairing in the bipyrazine ligand, and the appearance in the same spectrum of the vibrational patterns identified with bpy, bpy^-, and bpz^- argues for localized redox orbitals on individual ligands, with no delocalization. Moreover, one of the bpz^- peaks is observed to shift from 1211 to 1207 cm^{-1} on addition of the second electron into a bpy redox orbital, thus implying some interaction between bpz^- and bpy^-, possibly from changes in the Ru–bpz^- bond characteristics due to a change in Ru charge upon reduction of (primarily) bpy. The vibrational spectrum of the third reduction species is dominated by the spectrum of bpy^- throughout the visible excitation envelope; no evidence for bpz^- was found when either 20.1 $\times 10^3$ or 18.9 $\times 10^3$ cm^{-1} laser irradiation was used.

(42) Balk, R. W.; Stufkens, D. J.; Crutchley, R. J.; Lever, A. B. P. *Inorg. Chim. Acta* **1982**, *64*, L49.

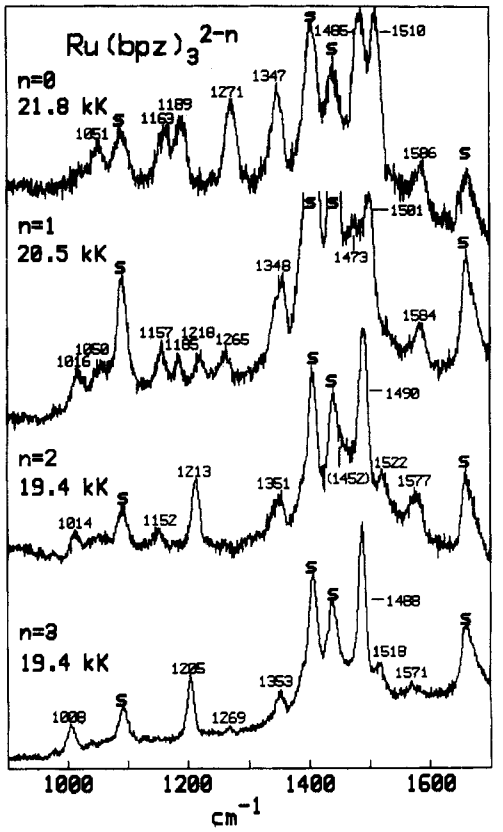

Figure 6. Resonance Raman spectra for the reduction products of $[Ru(bpz)_3]^{2-n}$ in DMF (1 kK = 1000 cm^{-1}; S = solvent peak).

C. $[Ru(bpz)_2(bpy)]^{2-n}$ (n = 0–3). Even at the highest visible energy of the Ar^+ ion laser (21.8×10^3 cm^{-1}), only the vibrational spectrum of bpz is observed for the unreduced complex (compare Figure 5 to Figure 6), consistent with the presence of two bpz ligands and a weaker MLCT absorption of the bpy ligand at a higher energy (24×10^3 cm^{-1}). After an electron is added, some bpy vibrations appear (1489, 1559, and 1599 cm^{-1}; Figure 5), implying a red shift of the MLCT, allowing the bpy modes to receive resonance enhancement. After two electrons have been added, the bpy modes become quite prominent, implying a further shift of the MLCT band. More striking, however, is the gradual shifting of the modes associated with bipyrazine. Some examples of this shifting for the $n = 0 \rightarrow n = 2$ sequence include the following peaks: 1510 → 1497 (−13) → 1479 (−18) cm^{-1}, 1272 → 1271 (−1) → 1266 (−5) cm^{-1}, and 1483 → 1470 (−13) → 1454 (−16) cm^{-1} (only seen for 18.9×10^3 cm^{-1} excitation), where the numbers in parentheses show the shift from the previous redox species. As electrons are added, a new peak (1216 (n = 1) → 1208 cm^{-1} (n = 2)) associated with bipyrazine is noted, as well as a change in the relative intensities of the bipyrazine peaks. While the presence of this new peak only in the reduced vibrational spectra may represent a vibrational of a separate bpz^- and hence imply a localized description of the redox orbital, the continuous shifting of the bands would suggest delocalization of the redox orbitals of the bipyrazines, with the "new" peak receiving resonance enhancement only from the $\pi^* \rightarrow \pi^*$ absorption and not from the MLCT absorption. The different enhancement from the $\pi^* \rightarrow \pi^*$ absorption vs. the MLCT absorption would also be expected to change the relative intensities of the other vibrational peaks. The resonance Raman spectrum for the three-electron-reduction product shows enhancement dominated by peaks associated with bpy^- (e.g. 1156, 1485, 1502, and 1562 cm^{-1}). These peaks are all within ~7 cm^{-1} of those for bpy^- as found in the RR spectra for $[Ru(bpy)_3]^{1+,0,1-}$ (1162, 1486, 1505, and 1558 cm^{-1}),[23] with the small shift attributed to a perturbation from different Ru–bpy bonding in the presence of bpz ligands. One peak in the n = 3 species that is associated with bipyrazine (1201 cm^{-1}) does appear in the spectrum when 18.9×10^3 cm^{-1} laser irradiation is used,

showing a further shift from its 1208-cm^{-1} position in the $n = 2$ species. A redox electron, even when added to a bpy ligand, seems to affect the vibrational frequency of the bipyrazines.

D. $[Ru(bpz)_3]^{2-n}$ ($n = 0$–3). The RR spectrum for the $(bpz)_3$ complex, shown in Figure 6, again demonstrates the shifting of vibrational frequencies as electrons are added, both in DMF and in Me_2SO. In addition to the peaks mentioned for the $(bpz)_2$ complex, the peak at 1586 → 1584 (−2) → 1577 (−7) → 1571 (−6) cm^{-1} also displays this shifting. The apparent change in relative intensity of the peaks, as well as the appearance of new peaks (1218 ($n = 1$) and 1522 cm^{-1} ($n = 2$)), may be attributable to a change in enhancement from MLCT absorption to $\pi^* \rightarrow \pi^*$ absorption rather than to the existence of distinct bpz^- ligands. In fact, the number of vibrational peaks (no more than 10 peaks clearly visible) in the intermediate redox products ($n = 1, 2$) is not inconsistent with the presence of only one vibrational chromophore,[43] in contrast to the two vibrational chromophores expected in a localized system. Where comparisons of bpz modes can be made, the vibrational spectrum of the two-electron-reduced species for the $(bpz)_2$ complex is very similar to the vibrational spectrum of the three-electron-reduced species for the tris complex, as expected since both cases have essentially one added electron per bpz ligand. Futhermore, the frequencies of the RR peaks for the one-electron-reduction product of the $(bpz)_2$ complex (Figure 5), with an average of half of an electron per ligand, are between those for the one- and two-electron-reduction products of the tris compound (one-third and two-thirds of an electron per ligand, respectively; Figure 6): 1497 (bis) vs. 1490 and 1501 cm^{-1} (tris); 1470 (bis) vs. 1452 and 1475 cm^{-1} (tris); and 1216 vs. 1213 and 1218 cm^{-1} (tris). Although such results are expected for a delocalized system of redox orbitals, the bpz vibrational sensitivity merely to the overall charge of the complex has been mentioned above for $[Ru(bpz)(bpy)_2]^+ \rightarrow [Ru(bpz)(bpy)_2]^0$, in which no delocalization is postulated.

One mechanisms besides delocalization for vibrational shifting have been observed previously and may be operative in these molecules. π back-bonding has been responsible for 10-cm^{-1} shifts in previous cases,[31-33] and such an effect may contribute in the reduced bpz complexes. Moreover, the total shift of bpz modes upon complete reduction is generally less than 20–30 cm^{-1}, as compared to ~50 cm^{-1} for modes associated with bpy,[27,44,45] and a varying degree of electron sharing with solvent is possible, especially since the basicity of the peripheral nitrogens of the bpz ligand increases upon reduction[46] and nucleophilicity of even the unreduced species has been demonstrated to red-shift absorption bands and increase π back-bonding upon addition of BF_3 to an aqueous solution of the complex.[47,48] While the shifting of the vibrational peaks occurred in both DMF and Me_2SO, the lack of solubility of the reduction products or even the unreduced species hampered investigation in other solvents. However, even with these alternatives, the RR data taken alone argue for delocalized redox orbitals between the bpz ligands.

III. Electron Spin Resonance (ESR). In contrast, though, a recent ESR study of the reduction products of $[Ru(bpz)_3]^{2-n}$ [40] and the near-IR absorption spectra reported here seem to support a localized description of the redox orbitals of the $(bpz)_3$ complex for the first two reduction products. The ESR study noted typical ruthenium diimine behavior for the one- and two-electron-reduction products, including temperature-dependent line width broadening associated with electron hopping from a reduced ligand to an unreduced ligand, and hence suggests a localized redox orbital. Extending that study, the ESR spectrum of the two-electron-reduction product $[Ru(bpz)_3]^0$ was recorded in a frozen DMF matrix (90–185 K); if the redox electrons were delocalized throughout the molecule and were no longer spatially isolated, there must be magnetic coupling between them to give either an $S = 0$ or $S = 1$ species, and this coupling should be detectable in a frozen matrix. An ESR signal persists even in fluid solution, and from the small g shift and different temperature dependence of the line width compared to that of the one-electron-reduction product, this signal can not be attributed merely to some one-electron impurity present in an otherwise $S = 0$ system. In frozen samples, the signal grows in intensity as the temperature is lowered from 185 to 90 K, but the g factor, shape, and line width remain unchanged. From Figure 7, the X, Y, and Z components expected for a triplet-state ESR spectrum[49-51] are not seen, with an ESR spectrum with g factor anisotropy[24,52] typical of doubly reduced ruthenium diimines appearing instead. This type of spectrum has been interpreted as indicating essentially magnetically noninteracting redox electrons, each having spin $^1/_2$ character.[24,51] Support for this interpretation is the lack of any signal at half-field ($\Delta M_s = \pm 2$ transitions) in the frozen matrix, as expected for a triplet-state ESR spectrum.[49-51] Furthermore, the g factor observed ($g = 1.995$), as well as the narrow line width in Figure 7, is inconsistent with assigning much ruthenium–metal character to the redox orbitals as would be likely in a delocalized orbital description, since the ruthenium would shift the g factor from the "free-electron" value typical of organic radicals and, through hyperfine splitting from the $^5/_2$ nuclear spin of ^{99}Ru and ^{101}Ru isotopes (combined 30% natural abundance),[40] broaden the peak-to-peak separation. The conclusion of redox orbital localization similar to that seen in other ruthenium diimine systems seems necessary from the ESR data, at least through the first two reduction products.

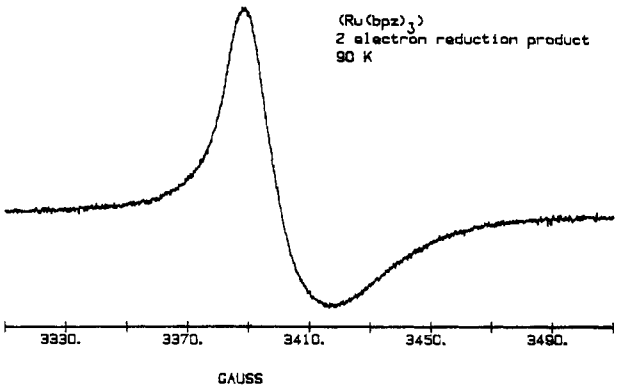

Figure 7. Low-temperature ($T = 90$ K) ESR spectrum of the two-electron-reduction product $[Ru(bpz)_3]^0$ in DMF. Microwave frequency = 9.55 GHz.

Conclusions

From the UV absorption spectra and the RR results for the redox series of $[Ru(bpm)_3]^{2-n}$, the redox orbitals are localized on single ligands through the first four added electrons. Furthermore, from the CV, UV–vis, and RR results, the mixed-ligand bpy–bpz complexes also possess bpy redox orbitals localized from the bpz redox orbitals. Localization of redox orbitals between the bpz ligands, at least for the first two reduction products, is suggested by the low-temperature ESR and the appearance of IVCT absorption bands for the $(bpz)_3$ complex. However, a satisfying interpretation of the UV and RR spectra for the series consistent with this conclusion is not reached.

(43) Measurable depolarization ratios indicate only a_1 modes are present in the bpz complexes (consistent with all other diimine complexes studied), and in comparison to the 11 a_1 modes observed for the bpy ligand in the frequency range examined,[25] only 10 modes are expected for a bipyrazine vibrational chromophore.

(44) Bradley, P. G.; Kress, N.; Hornberger, B. A.; Dallinger, R. F.; Woodruff, W. H. *J. Am. Chem. Soc.* **1981**, *103*, 7441.
(45) Forster, M.; Hester, R. E. *Chem. Phys. Lett.* **1981**, *81*, 42.
(46) Ernst, S.; Kaim, W. *J. Am. Chem. Soc.* **1986**, *108*, 3578.
(47) Dodsworth, E. S.; Lever, A. B. P.; Eryavec, G.; Crutchley, R. J. *Inorg. Chem.* **1985**, *24*, 1906.
(48) Crutchley, R. J.; Kress, N.; Lever, A. B. P. *J. Am. Chem. Soc.* **1983**, *105*, 1170.
(49) Wertz, J. E.; Bolton, J. R. In *Electron Spin Resonance: Elementary Theory and Applications*; McGraw-Hill: New York.
(50) Brown, I. M.; Weissman, S. I. *J. Am. Chem. Soc.* **1963**, *85*, 2528.
(51) Brown, I. M.; Weissman, S. I.; Snyder, L. C. *J. Chem. Phys.* **1965**, *42*, 1105.
(52) Motten, A. G.; Hanck, K.; DeArmond, M. K. *Chem. Phys. Lett.* **1981**, *79*, 541.

Acknowledgment is made to the donors of the Petroleum Research Fund, administered by the American Chemical Society, and to the National Science Foundation (Grant No. CHE-8507901) for support of this research.

Registry No. $[Ru(bpm)_3]^{2+}$, 80263-32-7; $[Ru(bpm)_3]^{+}$, 109468-63-5; $Ru(bpm)_3$, 109468-64-6; $[Ru(bpm)_3]^{-}$, 109468-65-7; $[Ru(bpz)(bpy)_2]^{2+}$, 85335-53-1; $[Ru(bpz)(bpy)_2]^{+}$, 93462-10-3; $Ru(bpz)(bpy)_2$, 93462-18-1; $[Ru(bpz)(bpy)_2]^{-}$, 93461-91-7; $[Ru(bpz)_2(bpy)]^{2+}$, 85335-51-9; $[Ru(bpz)_2(bpy)]^{+}$, 93462-11-4; $Ru(bpz)_2(bpy)$, 93462-19-2; $[Ru(bpz)_2(bpy)]^{-}$, 93461-92-8; $[Ru(bpz)_3]^{+}$, 75523-97-6; $Ru(bpz)_3$, 75523-95-4; $[Ru(bpz)_3]^{2+}$, 75523-96-5; $[Ru(bpz)_3]^{-}$, 75523-94-3; $[Ru(bpm)_3]^{2-}$, 109468-66-8; $[Ru(bpy)_3]^{2+}$, 15158-62-0; $[Ru(bpy)_3]^{+}$, 56977-24-3; $Ru(bpy)_3$, 74391-32-5; $[Ru(bpy)_3]^{-}$, 56977-23-2.

Contribution from the Department of Chemistry, Texas A&M University, College Station, Texas 77843

Surface Coordination Chemistry of Noble-Metal Electrodes. Hydrogen/Iodine Ligand (Adsorbate) Substitution at Smooth Polycrystalline Platinum

Jose F. Rodriguez, Beatriz G. Bravo, Thomas Mebrahtu, and Manuel P. Soriaga*

Received January 23, 1987

Adsorbate (ligand) displacement/substitution has been found to occur between iodine and hydrogen at smooth polycrystalline platinum electrodes in aqueous acid, neutral, or base electrolyte; experimental measurements were based upon thin-layer electrochemical methods. The iodine/hydrogen substitution reaction is a two-electron redox-activated process, the mechanism of which appears to depend upon the pH of the solution. In the absence of an applied potential, iodine is the only species present on the Pt surface. When a negative potential is applied in the vicinity of the hydrogen evolution reaction, chemisorbed iodine is progressively desorbed as iodide ions accompanied by the immediate chemisorption of protons as hydrogen atoms; when the potential is subsequently made positive, the reverse displacement reaction occurs in which hydrogen is oxidatively desorbed as protons accompanied by the oxidative chemisorption of iodide as iodine. In acid media, iodine desorption occurs *after* evolution of molecular hydrogen; in basic solutions, iodine removal occurs *before* electrogeneration of hydrogen gas.

Introduction

Although the strong interaction of aqueous iodide at platinum electrodes had been reported in the past,[1] it has only recently been established that a spontaneous oxidation–reduction process occurs when a clean platinum surface is exposed to aqueous iodide or gaseous hydrogen iodide. In this process, (i) iodide ions are oxidized to form a chemisorbed monolayer of zerovalent iodine atoms, and (ii) protons or water molecules are reduced to produce hydrogen gas;[2,3] at single-crystal surfaces, the chemisorbed layer of iodine has been found to be highly ordered.[2] In acid solutions, the oxidative chemisorption of iodide may be represented by

$$I^-(aq) + H^+ \rightarrow I(ads) + {}^1/_2H_2(g) \quad (1)$$

In neutral or basic media, the reaction may be written as

$$I^-(aq) + H_2O \rightarrow I(ads) + OH^- + {}^1/_2H_2(g) \quad (2)$$

The heat of adsorption of iodine on Pt has been measured from thermal desorption experiments to be *at least* 30 kcal/mol;[2] this stability betrays the formation of strong metal–adsorbate bonds analogous to those in transition metal–halide complexes. The question as to whether iodine chemisorption on platinum can be represented as zerovalent iodine on zerovalent platinum [Pt–I(ads)] or as a univalent platinum–iodide complex [Pt(I)–I^-] is largely unsettled although a recent study based on X-ray photoelectron spectroscopy supports the Pt–I(ads) representation.[4]

The spontaneous iodide-to-iodine oxidation upon contact with the Pt surface along with reactions 1 and 2 implies two important aspects of the surface chemistry of smooth polycrystalline platinum with iodine: (i) The standard potential for the Pt–I/Pt–I^- or I(ads)/I^-(ads) redox couple is shifted to negative values relative to that of the $I_2(aq)/I^-(aq)$ couple; that is, in the surface-bound state, iodine is more stable than iodide. (ii) Reactions 1 and 2 may be reversed by the presence of molecular hydrogen; that is, under certain electrochemical or catalytic conditions, ligand (adsorbate) substitution or displacement reactions between iodine and hydrogen may occur. The investigation of these fundamental surface processes was the purpose of this study.

The results obtained here demonstrate that adsorbate substitution or displacement can be made to transpire between iodine and hydrogen at smooth polycrystalline platinum electrodes in aqueous acid, neutral, or base electrolyte in the presence of ample amounts of hydrogen and/or by the application of sufficiently negative potentials. The displacement reaction is a two-electron redox-activated process, the mechanism of which appears to depend upon the pH of the solution. In the absence of an applied potential, iodine is more stable on the surface. When a negative (cathodic) potential is applied in the vicinity of the hydrogen evolution reaction, chemisorbed iodine is progressively desorbed as iodide ions accompanied by the immediate chemisorption of protons as hydrogen atoms; when the potential is subsequently made positive (anodic), the reverse displacement reaction occurs: hydrogen is oxidatively desorbed as protons accompanied by the oxidative chemisorption of iodide as iodine. In acidic media, iodine desorption occurs *after* evolution of molecular hydrogen; in basic solutions, iodine removal occurs *before* electrogeneration of hydrogen gas.

Experimental Section

Experimental measurements were based on thin-layer voltammetric and coulometric methods.[5] Thin-layer electrodes and their advantages in surface chemical studies have been discussed previously.[6] Smooth

* To whom correspondence should be addressed.

(1) (a) Osteryoung, R. A. *Anal. Chem.* **1963**, *35*, 1100. (b) Hubbard, A. T.; Osteryoung, R. A.; Anson, F. C. *Anal. Chem.* **1966**, *38*, 692. (c) Horanyi, G.; Rizmayer, E. M. *J. Electroanal. Chem. Interfacial Electrochem.* **1977**, *83*, 367.
(2) (a) Felter, T. E.; Hubbard, A. T. *J. Electroanal. Chem.* **1979**, *100*, 473. (b) Garwood, G. A.; Hubbard, A. T. *Surf. Sci.* **1980**, *92*, 617. (c) Stickney, J. L.; Rosasco, S. D.; Salaita, G. N.; Hubbard, A. T. *Langmuir.* **1985**, *1*, 66.
(3) (a) Soriaga, M. P.; Hubbard, A. T. *J. Am. Chem. Soc.* **1982**, *104*, 2742. (b) Soriaga, M. P.; White, J. H.; Song, D.; Hubbard, A. T. *J. Phys. Chem.* **1984**, *88*, 2284. (c) Lane, R. F.; Hubbard, A. T. *J. Phys. Chem.* **1975**, *79*, 808.
(4) DiCenzo, S. B.; Wertheim, G. K.; Buchanan, D. N. E. *Phys. Rev. B: Condens. Matter* **1984**, *30*, 553.
(5) Hubbard, A. T. *Crit. Rev. Anal. Chem.* **1973**, *3*, 201. Hubbard, A. T. *Acc. Chem. Res.* **1980**, *13*, 177.
(6) Soriaga, M. P.; Hubbard, A. T. *J. Am. Chem. Soc.* **1982**, *104*, 2735, 2742, 3937.

0020-1669/87/1326-2760$01.50/0